Journal of Biomechanics 38 (2005) 1591–1597

JOURNAL OF BIOMECHANICS

www.elsevier.com/locate/jbiomech
www.JBiomech.com

Development and evaluation of an optimization-based model for power-grip posture prediction

Sang-Wook Lee, Xudong Zhang*

Department of Mechanical and Industrial Engineering, University of Illinois at Urbana Champaign, 1206 West Green Street, 140 Mechanical Engineering Building, Urbana, IL 61801, USA

Accepted 30 July 2004

Abstract

An optimization-based model for power-grip posture prediction was proposed. The model was based on the premise that the hand prehensile configuration in a power grip best conforms to the object shape. This premise was embodied by an optimization procedure that minimized the sum of distances from the finger joints to the object surface. The model was evaluated against data from an experiment that measured the grasp postures of 28 subjects having diverse anthropometry. The intra- and inter-person variabilities in grip postures were empirically assessed and used as benchmark values for model evaluation. The evaluation showed that the root-mean-square (RMS) values of angle differences between the predicted and measured postures had a 13.7° grand mean (across all joints, subjects, and two cylindrical handles grasped), whereas the RMS values of the inter- and intra-person variabilities in measured postures had grand means of 13.0° and 4.4°, respectively. The model can be readily generalized to the prediction of postures in power-grasping objects of different shapes, and adapted for testing alternative prehensile strategies or performance criteria.

Keywords: Power grip; Posture prediction; Optimization; Performance criteria

1. Introduction

There has been sustained investigative attention directed to the human hand from different perspectives and for various purposes, such as classification of hand manipulative movements (Bendz, 1974; Elliot and Connolly, 1984; Napier, 1956), understanding the central mechanisms of finger interaction during force production (Latash et al., 2002; Zatsiorsky et al., 2000), and analysis of synergistic finger movements during manipulative or gestic acts (Braido and Zhang, 2004; Fish and Soechting, 1992; Santello et al., 2002). In addition, a significant number of biomechanical models have been developed to facilitate or complement the experimental studies of hand kinematics and kinetics. Examples include models for predicting finger muscle or tendon forces during isometric hand functions (An et al., 1985; Armstrong and Chaffin, 1978; Chao et al., 1976, 1989; Sancho-Bru et al., 2001, 2003), for identifying characteristics of hand movements during grasping motion (Smeets and Brenner, 1999), and for estimating fingertip location and muscle excursion from measured finger poses (Biggs and Horch, 1999). However, models for predicting hand prehensile configurations are relatively sparse (Buchholz and Armstrong, 1992). Such models can provide a kinematic basis for further kinetic or dynamic modeling and prediction, and can also help gain better understanding of human prehensile behavior.

A kinematic model was proposed by Buchholz and Armstrong (1992) to evaluate the prehensile capabilities in power grip of a cylindrical object. In that model, the

*Corresponding author. Tel.: +1-217-265-8031; fax: +1-217-244-6534.
E-mail address: xudong@uiuc.edu (X. Zhang).

0021-9290/$ - see front matter © 2004 Elsevier Ltd. All rights reserved.
doi:10.1016/j.jbiomech.2004.07.024

location and orientation of the object relative to the hand are first estimated by a statistical model synthesized from experimental data; the grip posture of the hand is then determined by an algorithm that "wraps" the finger segments around the object with the given hand position relative to the object. Since one major indeterminate aspect (i.e., the location and orientation of the object relative to the hand) of a grip configuration is not predicted per se, the applicability of the model remains limited. More importantly, the model does not support a general framework that allows evaluation of alternative grip strategies or performance criteria.

A much desired hand grip configuration model should simulate how the hand negotiates with an object, determining both the segmental angles and hand–object contacts, given the hand anthropometry and object geometry information. A general performance criterion governing human grip postural behavior would be the theoretical foundation of such a model. The human grasping motions (which terminate in grip postures) do appear to be "objective-oriented." That is, the pattern of the grip is dictated not only by the shape or size of the object but also by the intended activity (Jeannerod, 1997). For example, in a pinch grip which requires precision, the thumb and one or more of other fingers oppose to maintain stability. In a power grip, fingers are flexed to encircle the object to generate maximum grip force while minimizing concentrated mechanical stress (Napier, 1956).

The purpose of this work was to develop a new general biomechanical model for power-grip posture prediction and validate the model using experimental data acquired through in vivo measurement. The experimental data were also used to empirically derive two parameters, segment length and thickness, necessary for constructing the model. The model was sought to be general and optimization-based, with the objective function formulated as a performance criterion mathematically interpreting the theorized goal of a power grip.

2. Methods

2.1. Experimental database

An experiment was conducted to establish a database for the development and validation of the intended grip posture prediction model. Twenty-eight subjects (14 males and 14 females; average $\pm$ SD age: 23.6 ± 3.3 years), representing a wide range of anthropometry, participated in the experiment. None had any musculoskeletal discomfort or abnormality at the time of experiment. All subjects were right-handed, and their hand lengths, measured as the distance from the tip of digit 3 to the dorsal groove between the lunate and capitate bones, ranged from 142.4 to 182.5 mm. The average ($\pm$SD) hand lengths for the male and female subjects were 163.4 ($\pm$9.49) and 152.5 ($\pm$7.82) mm, respectively. Subjects were asked to perform right-hand motions of grasping two vertically oriented cylindrical handles, 45 and 50 mm in diameter. They began the motions in a consistent seated posture with the torso upright, the right upper arm approximately vertical and forearm horizontal on an armrest, the fingers in natural full extension (abduction–adduction not specified), and the palm facing medially. Note that the seat and armrest heights could be adjusted separately. Both handles were 150 mm tall, and had a $150 \times 150\,\mathrm{mm}^2$ rectangular base whose height was adjustable and set to be even with the armrest. Subjects reached forward over a distance of approximately 25 cm to grasp the handles, without needing significant forearm pronation–supination and torso assistance. They were instructed to achieve a firm but comfortable grip as if they were operating a manual control. Sufficient practice was allowed before the performance of actual trials that were measured. Reflective markers (5 mm in diameter) were attached on the dorsum of each subject's right hand at 21 surface landmarks (Fig. 1). A five-camera Vicon 250 motion capture system recorded the reflective marker coordinates at a sampling frequency of 120 Hz during the grasping motions, and then exported the three-dimensional (3D) coordinate data. Note that only the data for terminal static grip postures were needed in this study. The experimental protocol was approved by the Institutional Review Board of the University of Illinois at Urbana-Champaign, and informed consent was obtained from all the participants.

2.2. Kinematic representation of the hand

The hand excluding the thumb was represented by a rigid linkage system incorporating 22 degrees of freedom (DOF): 1 DOF each at the eight interphalangeal (IP) joints, 2 DOF each at the four metacarpophalangeal (MCP) joints, and 6 DOF total for the metacarpals treated as a single "palm" rigid segment. Two key parameters of the linkage representation, the length and thickness of individual link segments, were derived based on the above-described surface marker data. The segment length was defined as the distance between the joint centers of rotation (CORs) at two ends of a segment, whereas the segment thickness relevant to grip posture modeling was the segment thickness at contact (STAC) with the object, which was defined as the shortest distance between a segment and the object surface in a stabilized grip posture (see t_j^i in Fig. 2). An algorithm that computes the finger flexion–extension COR location from measured surface marker coordinates by minimizing the time-variance of link lengths or inter-COR distances (Zhang et al., 2003) was first applied to the data. This algorithm effectively

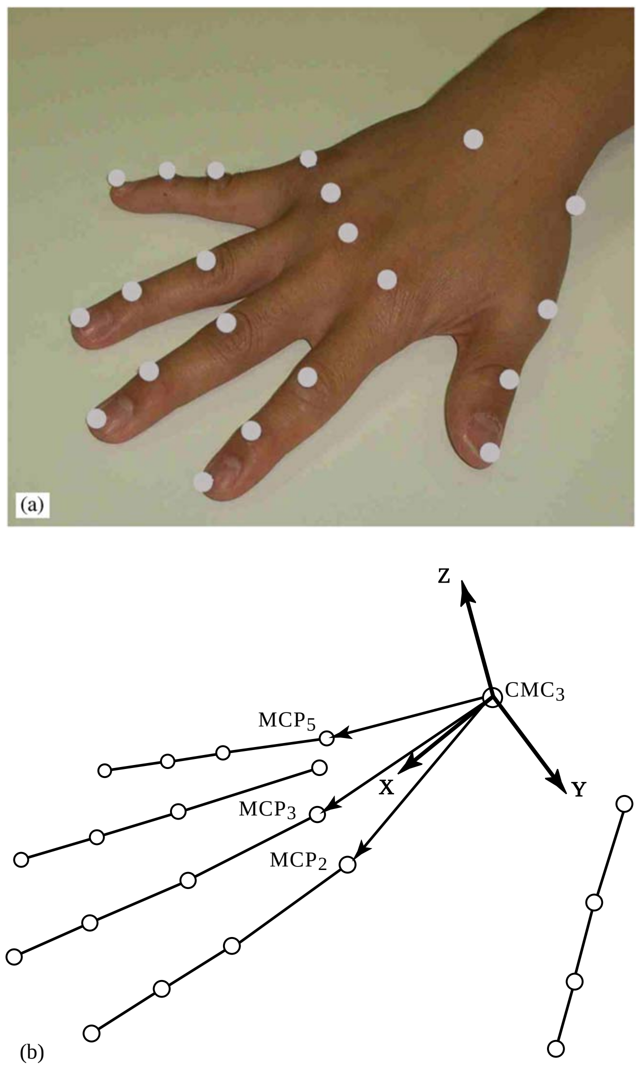

Fig. 1. (a) Retro-reflective markers (5 mm in diameter) were adhered to the dorsal aspect of the right hand at 21 surface landmarks; (b) A local coordinate system X–Y–Z was constructed using measured coordinates of the MCP2, 3, 5 and CMC3 markers. Note that the movements of the thumb markers were not analyzed in the current study.

determined the segment lengths. The STAC values were derived by fitting the object to a known grip configuration of the internal linkage while satisfying the constraints that the STAC values are proportional to the joint thickness measured in a posture with extended fingers.

The empirically obtained segment lengths and STAC values were expressed as ratios, respectively, to the hand length and corresponding joint thickness, and were statistically summarized. The statistical summary revealed that when the segment lengths were expressed as proportions of the hand length, the variation of the ratios across 28 subjects was small (coefficient of variation <0.1). To simplify the model input, the hand length was used to predict both the segment lengths and

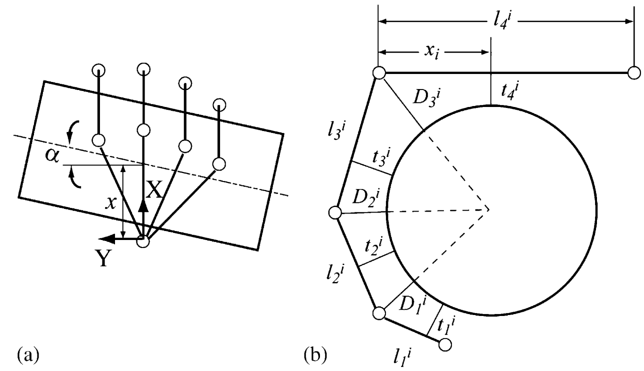

Fig. 2. Parameters in modeling the configuration of a power grip of cylindrical objects: (a) a top view; (b) a cross-sectional view.

STAC values. Although the correlation between the latter and the hand length was low (R^2 range: 0.35–0.50, Garrett, 1970), it was deemed that a systematic error in STAC across the joints would have a minimal effect on the angular prediction. The STAC values were nevertheless documented for more sophisticated prediction.

2.3. Optimization algorithm for power-grip posture prediction

An optimization routine for predicting power-grip postures was proposed, based on the premise that hand prehensile configuration should best conform to the shape of the object in a power grip. This premise is consistent with the stated goal or performance criterion of a power grip: to maximize the grip force while minimizing concentrated mechanical stress (Napier, 1956); when the hand configuration best conforms to the object shape, the contact area between the palm-side soft tissue and the object is most expanded and the forces exerted on the finger segments are most evenly distributed. It was embodied by an optimization routine that minimized the objective function as the summation of distances from the hand linkage joints to the object surface. Mathematically, the general objective function to be minimized was formulated as follows:

$$f = \sum_{i=2}^{5} \sum_{j=1}^{3} D_j^i \left[\underline{P}, \underline{H}, S(\underline{p}) \right], \tag{1}$$

where D_j^i is the distance from the COR of joint j in digit i to the object surface; $\underline{P}$ is the parameter set that defines the relative position of the hand to the object; $\underline{H}$ is the set of the hand dimension parameters including segment length and thickness values; and $S(\underline{p})$ is the mathematical representation of the object contour as a function of spatial parametric variable set $\underline{p}$.

Once the relative position of the hand to the object ($\underline{P}$) is given, the grip configuration is determined by wrapping the finger segment chain around the object while meeting the STAC constraint. Thus, the prediction problem is equivalent to finding the position parameter set $\underline{P}$ that results in a minimal f for the given hand dimension $\underline{H}$ and object contour $S(\underline{p})$:

$$\underline{P} = \arg\min_{\underline{P}} f = \arg\min_{\underline{P}} \sum_{i=2}^{5}\sum_{j=1}^{3} D_j^i[\underline{P}, \underline{H}, S(\underline{p})]. \quad (2)$$

The above general formulation can be specified for predicting postures of gripping a cylindrical object. Note that the position of hand ($\underline{P}$) can be described by two variables x and α for the grip postures of cylindrical object (Fig. 2). The hand dimensions $\underline{H}$ (lengths and thicknesses of the finger segments) can be represented as a set of functions of the hand length, as described earlier in Section 2.2. For a cylindrical object, the contour $S(\underline{p})$ can be characterized simply by its radius. Then Eq. (2) takes a more specific form as

$$\begin{aligned}(x, \alpha) &= \arg\min_{x,\alpha} f \\ &= \arg\min_{x,\alpha} \sum_{i=2}^{5}\sum_{j=1}^{3} D_j^i[x, \alpha, R, L_{\mathrm{h}}],\end{aligned} \quad (3)$$

where x and α denote the translational and rotational parameters determining the relative position of the cylinder with respect to the hand, R the radius of the cylinder, and L_{h} the hand length. The distance value D_j^i is formulated based on the mathematical representation of the cylindrical object contour. A detailed mathematical description of this function D_j^i for the grip of a cylindrical object is presented in Appendix A.

The prediction problem is equivalent to finding the position and orientation of the hand that result in a minimal value of objective function f for the given cylinder size and hand length.

2.4. Model performance evaluation

The intra- and inter-person variabilities in grip postures were empirically assessed and used as benchmark values for model performance validation. The intra-person variability was defined as the difference in joint angles for a given grip between repeated trials performed by the same subject. The inter-person variability was defined as the difference in joint angles of a given grip performed by subjects with similar hand lengths. To assess the inter-person variability, data for nine pairs of subjects (pair-wise hand length difference < 5 mm) selected out of the database were utilized.

Root-mean-square (RMS) values were computed to quantify these variabilities as well as the differences between the model-predicted and measured angles. The latter quantified the model prediction error. In addition, to examine possible bias (consistent over- or under-prediction) in the model, the mean and standard deviation of joint angle differences between the prediction and measurement were also calculated.

3. Results

The magnitude of inter-person variability is much greater than that of intra-person variability (Tables 1 and 2). For postures of gripping the smaller cylinder ($R = 45$ mm), the maximum RMS value is 10.37° for the intra-person variability, and 24.45° for the inter-person variability (Table 1); the grand mean of the RMS differences across all digits and joints is 5.00° for the intra-person variability, and 12.39° for the inter-person variability. For the larger cylinder ($R = 50$ mm), the maximum RMS value is 6.60° for the intra-person variability, and 28.45° for the inter-person variability (Table 2); the grand mean of the RMS differences across all digits and joints is 3.79° for the intra-person variability, and 13.52° for the inter-person variability. The variability, either inter- or intra-person, is substantially greater in the MCP joint than the other joints. However, there appears to be a tendency of reduced intra-person variability in the MCP joint angle in grasping the larger size cylinder.

The prediction errors of the proposed model, quantified as RMS values, were greater than the inter-person variability at the distal interphalangeal (DIP) and proximal interphalangeal (PIP) joints, particularly at the latter, but smaller at the MCP joints (Table 3). Across the four digits, the greatest error occurred at

Table 1
RMS values (deg) of the intra- and inter-person variability in grip posture for the cylinder of smaller size ($R = 45$ mm)

Digit	Intra-person ($n = 28$)			Inter-person ($n = 9$)		
	DIP	PIP	MCP	DIP	PIP	MCP
2	5.46	2.48	5.03	7.10	6.44	18.73
3	5.29	2.31	5.89	8.13	6.65	17.00
4	4.40	2.27	6.75	11.41	9.18	18.97
5	3.83	5.92	10.37	8.40	12.26	24.45

Table 2
RMS values (deg) of the intra- and inter-person variability in grip posture for the cylinder of larger size ($R = 50$ mm)

Digit	Intra-person ($n = 28$)			Inter-person ($n = 28$)		
	DIP	PIP	MCP	DIP	PIP	MCP
2	3.57	3.62	3.46	6.69	7.36	22.15
3	2.92	1.97	3.59	7.70	4.71	20.19
4	3.75	2.41	4.43	11.14	8.01	23.79
5	4.90	4.25	6.60	8.40	13.69	28.45

digit 5. The grand mean of the RMSE across all digits and joints is 14.15° for 45 mm cylinder, and 13.21° for the 50 mm cylinder. The mean and standard deviation of the angle difference (which could be positive or negative) do not seem to suggest any pattern of bias (Table 4). The error dispersion as measured by the standard deviation is comparable to what was reported for an existing model (Buchholz and Armstrong, 1992).

Data for two parameters, the internal segment length and STAC, was statistically summarized (Tables 5 and 6). The derived STAC values, when expressed as ratios to the corresponding proximal joint thicknesses and averaged across subjects, exhibited congruency across the fingers (Table 6). So did the ratios to the respective hand lengths (Table 7). However, the variation in the latter ratios was substantial.

4. Discussion

This work aimed to develop a mathematical model for predicting power-grip posture and to evaluate the model against experimental data acquired in vivo using surface measurement technology. The model was based on a general premise that the hand configuration in a power grip best conforms to the shape of the object. This premise was embodied as an optimization procedure with the objective function of minimizing the sum of distances from finger joints to the surface of the object. The model was illustrated by a formulation for predicting postures of grasping relatively simple cylindrical handles. Accordingly, the experiment for model validation entailed the performance of cylindrical handle grasps by anthropometrically diversified subjects.

The proposed modeling framework can be generalized to the prediction of the grip postures in interacting with objects of more complicated shape, as long as the object geometry can be mathematically specified or even approximated. This generality was lacking in a previous model (Buchholz and Armstrong, 1992), but is believed to be a necessity for the model to be practically useful in applications such as computer-assisted clinical evaluation and tool design. The model is also readily expandable for testing alternative hypothesized grip strategies or performance criteria as represented by various objective functions. In that regard, it is recognized that the proposed general objective function did not capture the varied prehensile strategies, and perhaps should be considered as the representation of an ideal or "optimal" strategy. Large inter-person variability in the grip postures was indeed evidenced, and two distinct general strategies were observed, one with and one without the palm completely attached to the cylindrical object. They were affected by how the thumb was positioned, and somewhat similar, respectively, to the diagonal volar grasp and transverse volar grasp as described by Buchholz and Armstrong (1992). We postulate that the proposed objective function well represented the first strategy but not the second (which was adopted by only a few subjects). This seems to concur with the observation that the model prediction was on an average the smallest for digit 2—the digit adheres to the object surface regardless of the grasp strategy. A rigorous test of this postulation remains an important step leading to an improved model.

Several sources of error may have contributed to the inaccuracy of the proposed prediction model. First of

Table 3
RMS values (deg) of the model prediction error

Digit	Smaller cylinder ($R = 45$ mm)			Larger cylinder ($R = 50$ mm)		
	DIP	PIP	MCP	DIP	PIP	MCP
2	8.66	15.36	14.52	7.90	13.15	15.96
3	15.33	11.36	16.00	11.56	9.36	13.64
4	10.83	10.05	15.47	11.08	9.92	15.46
5	17.47	14.76	19.95	16.57	13.90	20.02

Table 5
Mean values of the segment length/hand length ratios

	Digit			
	2	3	4	5
Distal phalange	0.1709	0.1740	0.1722	0.1553
Middle phalange	0.1713	0.1928	0.1963	0.1404
Proximal phalange	0.2822	0.3299	0.2978	0.2502

Table 4
Mean (SD) values of the model prediction error

Digit	Radius: 45 mm			Radius: 50 mm		
	DIP	PIP	MCP	DIP	PIP	MCP
2	2.22 (8.59)	−11.88 (9.99)	−3.63 (14.45)	1.22 (8.00)	−11.76 (6.03)	6.87 (14.78)
3	−9.19 (12.61)	8.93(7.21)	−11.69 (11.21)	−6.02 (10.13)	7.26 (6.06)	−2.83 (13.69)
4	5.46 (9.60)	−1.75 (10.17)	−5.87 (14.71)	3.10 (10.91)	1.28 (10.09)	2.42 (15.67)
5	−11.85 (13.19)	0.86 (15.14)	0.95 (20.47)	−11.80 (11.93)	−1.60 (14.16)	10.57 (17.44)

Table 6
Mean values of the STAC/joint thickness ratios

	Digit			
	2	3	4	5
Distal phalange	0.589	0.649	0.615	0.619
Middle phalange	0.405	0.403	0.370	0.429
Proximal phalange	0.198	0.223	0.282	0.275

Table 7
Mean values of the STAC/hand length ratios

	Digit			
	2	3	4	5
Distal phalange	0.0484	0.0469	0.0466	0.0525
Middle phalange	0.0628	0.0600	0.0613	0.0646
Proximal phalange	0.0948	0.0938	0.0907	0.1039

all, the variability in grip postures due to personal preferences is an inherent source of error. Overall, the prediction accuracy of the current model compared favorably with the inter-person variability and that of the existing model by Buchholz and Armstrong (1992). Some discrepancies also arose from the process of constructing the human hand linkage representation. For instance, segment lengths were predicted as proportions of the hand length based on regression analysis of measured data. Although the coefficients of variation of the ratio (<10%) well justified the prediction method, the discrepancy between the predicted and measured segment lengths was inevitable. The segment thicknesses at contact, as constraint parameters, were estimated by fitting the cylindrical objects to the measured postures while assuming a linear increase of the thickness in the distal–proximal direction. This estimation could not have been immune to error. The error may have been further amplified in the modeling, as the thickness values were predicted by the hand length mainly for simplicity and convenience.

Acknowledgements

This work was supported by Caterpillar Inc. and the National Science Foundation (DMI-0200143).

Appendix

A. Derivation of distance D_j^i for the grip posture of cylindrical object

The location and orientation of the cylindrical object with respect to the hand in a power-grip posture can be specified by two parameters: location variable x and orientation angle α (Fig. 2). For digit i, the distance from the contact point to MCP$_i$, $x_i(x, \alpha)$, is expressed as follows (Fig. 2a):

$$x_i(x,\alpha) = x + [y_{\mathrm{MCP}i} - y_{\mathrm{MCP5}}] + [y_{\mathrm{MCP}i} - y_{\mathrm{MCP5}}] \tan \alpha, \quad \text{(A.1)}$$

where $x_{\mathrm{MCP}i}$ and $y_{\mathrm{MCP}i}$ denote the x and y coordinates of MCP$_i$ in the local coordinate system built on the dorsal aspect of the hand.

The distance from jth joint in digit i, D_j^i can then be expressed as a function of $x_i(x, \alpha)$ as the following (see Fig. 2b):

$$D_1^i(x,\alpha,R,L_{\mathrm{h}}) = -R + \sqrt{(l_2^i - \sqrt{(R+D_2^i)^2 - (R+t_2^i)^2})^2 + (R+t_2^i)^2}, \quad \text{(A.2)}$$

$$D_2^i(x,\alpha,R,L_{\mathrm{h}}) = -R + \sqrt{(l_3^i - \sqrt{(R+D_3^i)^2 - (R+t_3^i)^2})^2 + (R+t_3^i)^2}, \quad \text{(A.3)}$$

$$D_3^i(x,\alpha,R,L_{\mathrm{h}}) = -R + x_i^2 / \sqrt{x_i^2 + (R+t_4^i)^2}, \quad \text{(A.4)}$$

where l_j^i denotes the length of the jth segment of digit i, t_j^i the thickness of the jth segment of digit i, and R the cylinder radius.

Note that the segment length l_j^i should be modified when the segments of a digit lie in a plane (the digit flexion–extension plane; plane D in Fig. 3) that is not perpendicular to the cylinder axis. Under such circumstances, the finger segments were projected to a plane perpendicular to the cylinder axis (plane C) and the distances are calculated using projected segment length

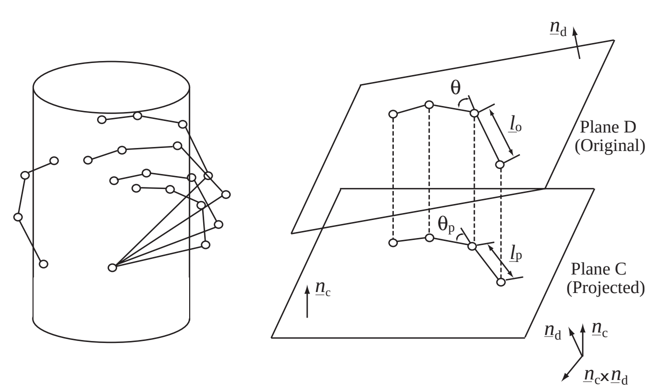

Fig. 3. When the segments of a digit lie in a plane (plane D) that is not perpendicular to the cylinder axis, the finger segments are projected onto a cross-sectional plane that is perpendicular to the cylinder axis (plane C). The projected finger segment length is a function of its original length and orientations of the planes $||\underline{l}_p|| = f(||\underline{l}_o||, \underline{n}_c, \underline{n}_d)$.

$||\underline{l}_\mathrm{p}||$ as follows:

$$||\underline{l}_\mathrm{p}|| = \sqrt{(||\underline{l}_\mathrm{o}||^2 - ||\underline{l}_\mathrm{o} \cdot (\underline{n}_\mathrm{c} \times \underline{n}_\mathrm{d})||^2) \cdot (\underline{n}_\mathrm{c} \cdot \underline{n}_\mathrm{d})^2 + ||\underline{l}_\mathrm{o} \cdot (\underline{n}_\mathrm{c} \times \underline{n}_\mathrm{d})||^2}, \tag{A.5}$$

where $\underline{n}_\mathrm{c}$ is the unit normal vector of plane C which is normal to the cylinder axis; $\underline{n}_\mathrm{d}$ the unit normal vector of plane D where segments of a digit lie; $\underline{l}_\mathrm{o}$ the original segment vector on plane D (digit plane); and $\underline{l}_\mathrm{p}$ the segment vector projected on plane C (cylinder cross-sectional plane).

Eqs. (A.2)–(A.4) can then be used in the prediction model with the original segment length l_j^i replaced by the projected segment length $||\underline{l}_\mathrm{p}||$. The last step of modification that should be taken is to calculate joint angles on the original digit plane (plane D). The joint flexion angle is calculated from the flexion angle on the plane C, θ_p, the original jth segment length l_j and projected jth segment length $l_{j\mathrm{p}}$ as follows:

$$\theta = \cos^{-1}\left(\frac{l_j^2 + l_{j+1}^2 - \left(l_{j\mathrm{p}}^2 l_{(j+1)\mathrm{p}}^2 - 2l_{j\mathrm{p}}^2 l_{(j+1)\mathrm{p}}^2 \cos\theta_\mathrm{p} - \left(\sqrt{l_j^2 - l_{j\mathrm{p}}^2} - \sqrt{l_{j+1}^2 - l_{(j+1)\mathrm{p}}^2}\right)^2\right)}{2l_j l_{j+1}}\right). \tag{A.6}$$

References

An, K.N., Chao, E.Y., Cooney, W.P., Linscheid, R.L., 1985. Forces in the normal and abnormal hand. Journal of Orthopaedic Research 3, 202–211.

Armstrong, T.J., Chaffin, D.B., 1978. An investigation of the relationship between displacement of the finger and wrist joints and the extrinsic finger flexor tendons. Journal of Biomechanics 1, 119–128.

Bendz, P., 1974. Systematization of the grip of the hand in relation to finger motor systems: a Kinesiological study using a new method for recording finger joint motions. Scandinavian Journal of Rehabilitation Medicine 6, 158–165.

Biggs, J., Horch, K., 1999. A three-dimensional kinematic model of the human long finger and the muscles that actuate it. Medical Engineering & Physics 21, 625–639.

Braido, P.N., Zhang, X., 2004. Quantitative analysis of finger motion coordination in hand manipulative and gestic acts. Human Movement Science 22, 661–678.

Buchholz, B., Armstrong, T., 1992. A kinematic model of the human hand to evaluate its prehensile capabilities. Journal of Biomechanics 25, 149–162.

Chao, E.Y., Opgrande, J.D., Axmear, F.E., 1976. Three-dimensional force analysis of finger joints in selected isometric hand functions. Journal of Biomechanics 9, 387–396.

Chao, E.Y., An, K.N., Cooney, W.P., Linscheid, R.L., 1989. Biomechanics of the Hand: A Basic Research Study. World Scientific, Singapore.

Elliot, J.M., Connolly, K.J., 1984. A classification of manipulative hand movements. Development Medicine and Child Neurology 26, 283–296.

Fish, J., Soechting, J.F., 1992. Synergistic finger movements in a skilled motor task. Experimental Brain Research 91, 327–334.

Garrett, J.W., 1970. Anthropometry of the hands of male air force flight personnel, AMRL-TR-69-42. Aerospace Medical Research Laboratory, Wright-Patterson AFB, Ohio.

Jeannerod, M., 1997. Grasping objects: the hand as a pattern recognition device. In: Hepp-Reymond, M.-C., Marini, G. (Eds.), Perspectives of Motor Behavior and its Neural Basis. Basel, Karger, pp. 19–32.

Latash, M.L., Li, S., Danion, F., Zatsiorsky, V.M., 2002. Central mechanisms of finger interaction during one- and two-hand force production at distal and proximal phalanges. Brain Research 924, 198–208.

Napier, J.R., 1956. The prehensile movements of the human hand. Journal of Bone and Joint Surgery 38, 902–913.

Sancho-Bru, J.L., Perez-Conzalez, A., Vergara, M., Giurintano, D.J., 2001. A 3D dynamic model of human finger for studying free movements. Journal of Biomechanics 34, 1491–1500.

Sancho-Bru, J.L., Perez-Conzalez, A., Vergara, M., Giurintano, D.J., 2003. A 3D biomechanical model of the hand for power grip. Journal of Biomechanical Engineering 125, 78–83.

Santello, M., Flanders, M., Soechting, J.F., 2002. Patterns of hand motion during grasping and the influence of sensory guidance. The Journal of Neuroscience 22, 1426–1435.

Smeets, J.B.J., Brenner, E., 1999. A new view on grasping. Motor Control 3, 237–271.

Zatsiorsky, V.M., Li, Z.M., Latash, M.L., 2000. Enslaving effects in multi-finger force production. Experimental Brain Research 131, 187–195.

Zhang, X., Lee, S.-W., Braido, P.N., 2003. Determining finger segmental centers of rotation in flexion-extension based on surface measurement. Journal of Biomechanics 36, 1097–1102.